SOLAR CHIMNEY AUGMENTED PASSIVE DOWNDRAUGHT EVAPORATIVE COOLING SYSTEM

Botha, DW, Dobson, RT

Department of Mechanical and Mechatronic Engineering, University of Stellenbosch, Stellenbosch, Private Bag XI, MATIELAND, 7602
Tel 27 (0)21 8084286, fax 27 (0)21 8084958, e-mail, rtd@sun.ac.za, coenraad@sun.ac.za

Abstract

Although passive evaporative cooling towers and chimneys have been successfully utilised for thousands of years their quantitative simulation based on thermofluid principles has not been fully developed and packaged such the their energy saving potential can be readily quantified. The object of this paper is to present a one-dimensional flow model of a small-scale model (100 mm diameter and about 3m high) of such a system. The system consists of a downdraught tower connected at the bottom to another tower or chimney that can be heated by solar energy. At the top of the downdraught tower is a structure containing wetted pads from which water can evaporate, cool down and in turn cool the air and thereby increase its density. At the bottom of the downdraught tower this now cooled air is channelled to the chimney which when heated will heat the air, decrease its density, and thereby contribute to enhancing the air flow through the system. The system is discretised into a number of control volumes. The equations of change describing the transient flow and heat and mass transfer are derived in finite difference form suitable for numerically solution using an explicit upwind formulation technique. The theoretical results are compared with the experimental results and were found to capture the physical behaviour of the system. It was thus concluded that, at least on a one-dimensional small scale that the theoretical model is reasonably accurate.

Keywords: Passive evaporative cooling, downdraught cooling, Mathematical modelling, Experimental validation, solar chimney,

1 Introduction

The use of natural draught towers to provide thermal comfort in buildings has for many years been recognised as a passive cooling strategy. For centuries wind-towers have been used in traditional Middle Eastern architecture to promote natural ventilation, occasionally making use of evaporative cooling (Errel, Pearlmutter & Etzion, 2007).

According to Barozzi et al. (1992) the need for passive cooling strategies is greatest in developing countries due to poor building technologies and limited financial resources. The reasoning behind this statement include the fact that modern building design in many cases has superseded indigenous architecture; the cost of imported materials and components along with increased fuel consumption required to cool buildings contributes to financial ruin. Nicol (2008) researched the integration of vernacular passive-cooling systems in modern buildings in Iran. He argues that in contrast to modern buildings, vernacular architecture is more adaptable to the environment according to principles evolved over generations. In the present context vernacular architecture refers to traditional building techniques developed over time to suit local needs.

Etzion et al (1997) state that it is often possible to harness natural energies and exploit the local climate to great advantage by adapting the architectural design of buildings rather than investing non-renewable energy to counteract the natural conditions. However, it is argued that climate conscious design requires a thorough understanding of the local climate and relevant strategies in order to achieve human comfort with a minimal investment of energy.

The development of design tools for passive cooling systems could potentially help to better understand the operation and integration of these systems in buildings.

Heating, ventilation and air conditioning (HVAC) systems are the major energy consumers in most industrial and commercial buildings (Tsal, 1999). It is estimated that HVAC system may contribute up to 30% of the initial building cost and 40% of the building's operating energy expense. Economic considerations often determine the viability of renewable energy strategies in practice. In order for renewable technologies to compete against conventional technologies the upfront and operational cost must be of the same magnitude as that of conventional approaches.

An example of a passive cooling strategy employs a passive downdraught evaporative cool tower (PDECT) in conjunction with a solar chimney (SC) to achieve thermal tempering in a structure. Figure 1 depicts the basic layout of a building with a solar chimney assisted passive downdraught evaporative cooling (SCAPDEC) system. The SCAPDEC system operates on the principle of buoyancy driven flow. Ambient air enters the downdraught tower and is cooled by the evaporation of water from wetted pads at the top of the downdraught tower (Pearlmutter et al., 1996).

Water vapour migrates from the pads to the surrounding air due to a concentration difference of water vapour at the air-water interface. This concentration difference is the driving force for mass transfer from the wetted pads to the surrounding air.
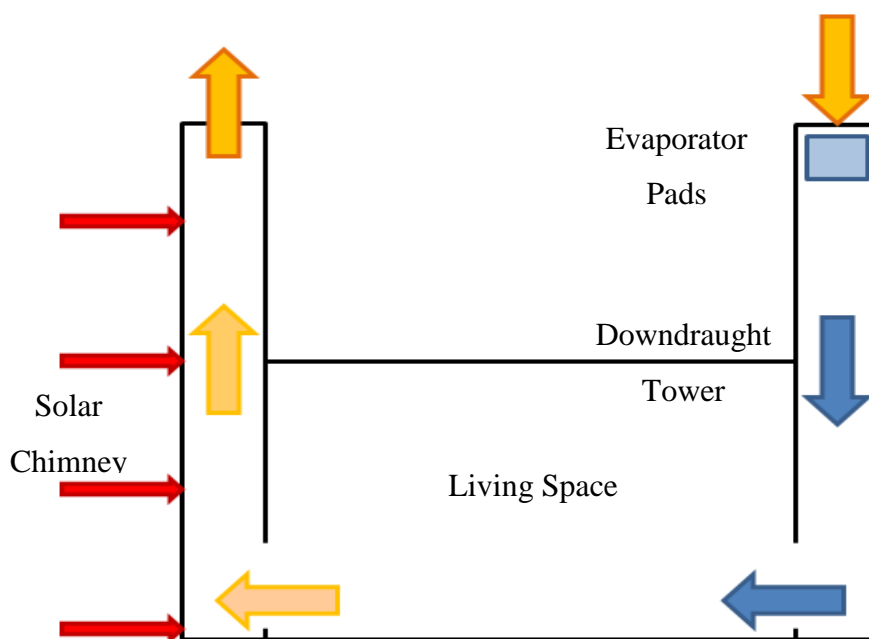

Figure 1 Solar chimney augmented passive downdraught evaporative cooling system

The mass transfer of water vapour from the surface of the wetted pads results in energy being transferred from the surface of the pads to the surrounding air. The removal of energy from the pad surface establishes a temperature difference between the pad surface and the surrounding air. This temperature is the driving force for heat transfer from the air (Cengel, 2006).

In the absence of wind, the cool, dense air travels along the downdraught tower due to buoyancy driven flow and enters the living space through vents. Depicted in Figure 1 is a solar chimney situated on the opposite side of the living space. The chimney walls are

heated by incident solar radiation resulting in heat transfer from the chimney walls to the air inside the chimney. The heated, less dense air rises in the solar chimney, drawing stagnant air from the living space and exhausting it to the environment. The aim of the buoyancy driven, natural air circulation system described above is to provide sufficient comfort to the occupants of the building at a reduced energy cost.

According to Cunningham, Mignon and Thompson (1987), the two towers may be operated in unison or separately for the case where ambient conditions are not favourable for the operation of one of the towers. It is suggested that the downdraught tower may operate alone at night while the solar chimney will operate alone under high humidity conditions.

The aim of this project is to develop a one-dimensional theoretical model to predict the performance of solar chimney augmented passive downdraught evaporative cooling systems. The proposed theoretical model will be validated by means of a small scale experimental model.

This report summarises the methodology followed, work done and findings made in developing a theoretical model to assimilate the operation of SCAPDEC systems. The basic layout of the report consists of the following sections; literature study; theory; results; discussion and conclusions; recommendations. A review of current modelling techniques for SCAPDEC systems along with a motivation for the current study is presented in the literature study. The theoretical model is developed firstly for the evaporation process and then for the remainder of the system. Next the experimental setup used for validating the theoretical model is explained. The data gathered through the theoretical and experimental analyses are then presented and discussed. The objectives of the project are met by drawing conclusions from a comparison of the experimental and theoretical data. Finally recommendations are made based on conclusions drawn from the theoretical and experimental comparison.

2 Experimental Set-up

The basic layout of the experimental SCAPDEC system is shown in figure 2 where the main sections of the experimental model corresponding to the sections to be incorporated into the theoretical model are the: evaporator section with removable evaporative cartridge, gradual contraction, downdraught tower, living space, solar chimney and diffuser. Additional components illustrated in figure 2 are the adjustable, conical inlet cone and air heater (hair dryer) incorporated into the solar chimney.

The evaporative cartridge consists of eight concentric, cotton cloth cylinders supported by a wire frame. The removable cartridge, shown in figure 3, is 300 mm high with an outer diameter of 400 mm and a radial spacing of 20 mm between successive cylindrical pads. The cotton cloth for the evaporative cartridge was selected based on a series of tests conducted by Dobson and le Grange (2009). The study investigated the rates of evaporation of water vapour into air for various commercially available, woven cotton specimens. The tests were conducted by partially immersing the ends of wetted cotton strips in separate containers filled with water. Water evaporates from the cottons strips while the pads are kept wet by drawing water from the container through capillary action. The rates of evaporation of the various specimens were compared by monitoring the water level in each container.
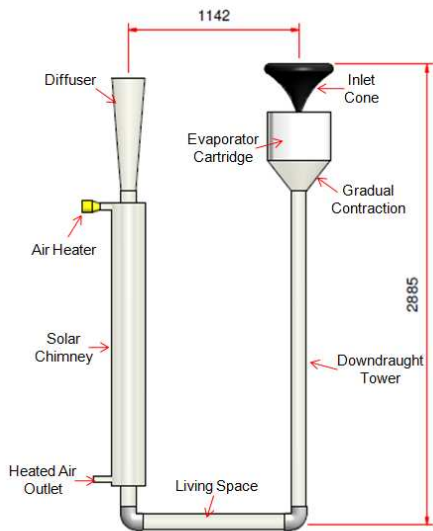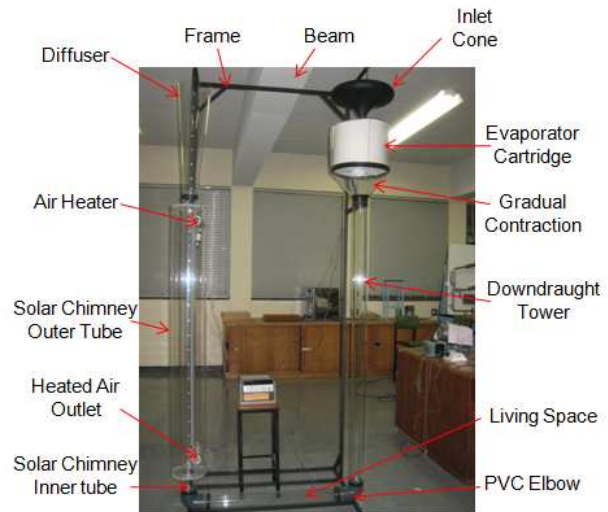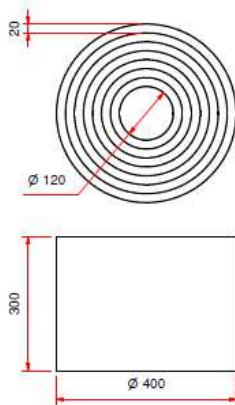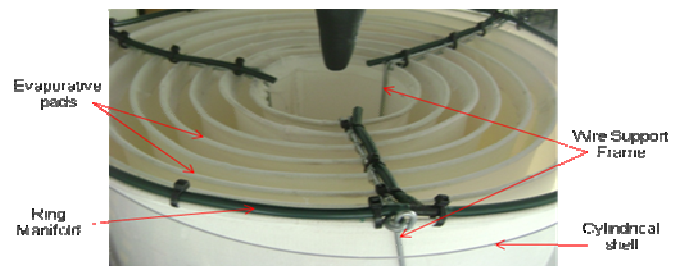
(a) Schematic layout   (b) Photograph of set-up in laboratory
Figure 2 SCAPDEC scale model layout diagram

(a)   (b)
Figure 3 Evaporator cartridge diagram (a) showing ring water supply manifold on evaporative cartridge (b)

Water is supplied to the evaporative pads through a ring manifold with three radial branches fixed to the top of the cartridge as shown in figure 3. Water is fed from a water reservoir through a drip system to the manifold. The drip system allows control over the water flow rate to the pads. The manifold can readily be disconnected from the drip system in order to remove the evaporator cartridge from the system.

The cartridge is seated inside a cylindrical, acrylic shell, also shown in figure 3. The shell has an inside diameter of 400 mm and a wall thickness of 1 mm and is connected to a gradual reducer reducing from 400 mm to 100 mm over a distance of 190 mm. The gradual reducer was formed from the same 1 mm thick acrylic sheet as the cylindrical shell, surrounding the evaporator cartridge.

The downdraught tower, living space and solar chimney essentially consist of three lengths of clear, acrylic tubing connected by means of PVC elbows. The acrylic tubing has an inner diameter of 94 mm and an outer diameter of 100 mm. Standard 90 mm bore PVC solvent-type elbows were bored to 100 mm in order to fit the non-standard size acrylic tube.

For the purpose of the laboratory SCAPDEC scale model the solar chimney was approximated by a simple tube-in-tube heat exchanger. The inner acrylic tube of 100 mm outer diameter is enclosed inside an acrylic cylinder with an outer diameter of 230 mm and a wall thickness of 1 mm. Both ends of the outer cylinder are capped with annular discs manufactured from 1 mm thick acrylic sheet. Heated air is supplied through a 40 mm (inside diameter) PVC pipe, to the top of the annular space between the two cylinders, by means of an 1800 W hairdryer with two power settings. The warm air is extracted at the bottom of the annular space through another 40 mm diameter PVC exhaust tube. Heat transfer takes place from the annular space through the inner tube, heating the air-vapour mixture inside the inner tube. At the top, the inner tube of the "solar chimney" heat exchanger is connected to a diffuser section. The diffuser expands from a diameter of 100 mm at its base to a diameter of 220 mm over a length of 700 mm.

A frame was constructed from mild steel to support the SCAPDEC model in the laboratory. The design of the frame allows for the removal of the downdraught tube with gradual contraction and evaporator section, living space, solar chimney and diffuser. A modular design is implemented to enable further investigation of either a solar chimney or passive downdraught evaporative cool tower. It would also be possible to interchange the living space, currently being modelled as horizontal pipe, with a setup that is more representative of an actual building. This setup might include a cooling load and flow obstructions as would be found in an actual building. Figure 2(b) displays the completed SCAPDEC laboratory scale model with frame.
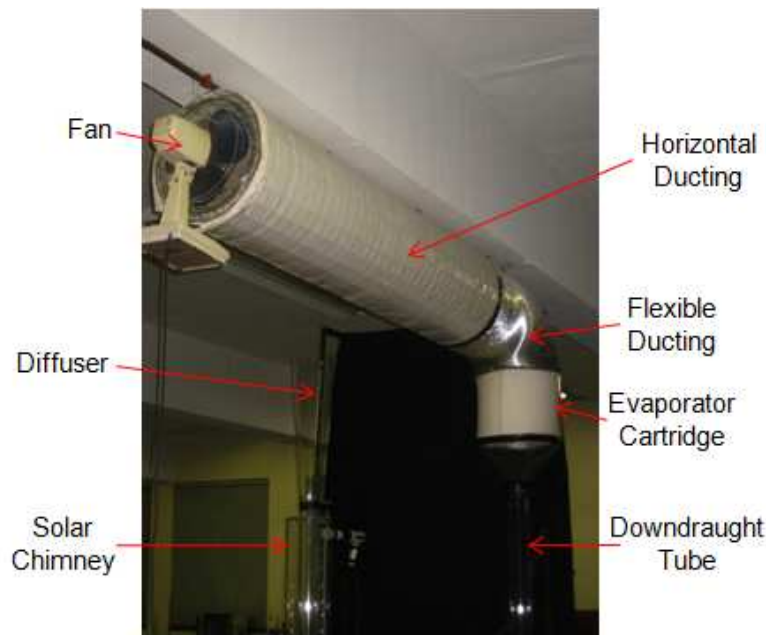

Figure 4 Forced draught experimental setup

To prevent hot, humid air exhausted from the SCAPDEC model being drawn back into the system during testing, the model was placed underneath the roof beam shown in figure 4. A cardboard sheet (not shown) was suspended 1 m below the beam to further separate the inlet and outlet of the SCAPDEC model.

A forced draught experimental setup that can be attached to the SCAPDEC system was designed. This was done to validate the theoretical model at higher volumetric flow rates. The forced draught experimental setup makes use of a fan to force air through a horizontal duct into the SCAPDEC model. Figure 4 shows the fan and horizontal duct suspended from the laboratory ceiling. The horizontal duct is connected to the top of the evaporator cartridge through an elbow fashioned from flexible ducting. The light weight horizontal ducting consists

of a layer of cotton cloth and plastic sheet wrapped around a 400 mm diameter cylindrical wire grid frame. The length of ducting was sourced from the PDECT experimental tower used by le Grange (2009). The forced draught setup is attached to the SCAPDEC model by firstly removing the adjustable inlet cone from the model. Once the SCAPDEC model is positioned under the horizontal duct the length of flexible ducting may be attached to the acrylic shell at the top of the evaporative cartridge. Duct tape was used to seal the joint between the flexible ducting and the acrylic shell.

3. Theory

The solar chimney assisted passive downdraught evaporative cooling loop is represented by the control volume discretisation scheme shown in Figure . The loop consist of the six distinct axially symmetric sections along its length, namely the evaporator L_1, gradual contraction L_2, downdraught tube L_3, living space L_4, up-draught heating tube L_5 and diffuser section L_6.

Each section in the loop has a predefined length L and number of control volumes N. The length of specific control volume dx is therefore the length of the section wherein the control volume resides divided by the number of control volumes in the section. In the evaporator each lengthwise control volume is further subdivided into annular control volumes formed by concentric, cylindrical evaporator pads.
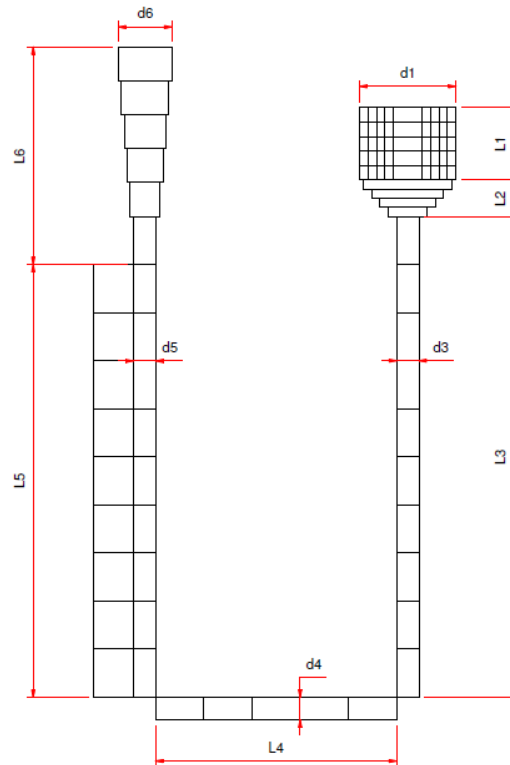

Figure 5 SCAPDEC control volume discretisation scheme

An explicit solution method is used to solve the finite difference equations, for the conservation of mass, conservation of energy and conservation of momentum in each control volume, in order to arrive at the new conditions in each control volume after a small but finite time step Δt.

In order to present a one dimensional theoretical model of a SCAPDEC system it was necessary to simplify the problem by making the following assumptions and approximations:

- A uniform property distribution is assumed in each control volume. This implies that the diffusion rate of water vapour across a control volume is neglected.

- The air-water vapour mixture obeys the ideal gas relation. This assumption results in negligible error for temperatures under 50°C and water vapour pressures less that 12.3 kPa (Cengel and Boles, 2007).

- The model includes only buoyancy driven ventilation and wind induced ventilation is not considered.

- The Boussinesq approximation is applied in solving equations for the conservation of momentum. The Boussinesq approximation implies that fluctuations in density which result primarily from thermal effects as opposed to pressure effects. Furthermore, in the equations for rate of change of momentum and mass, density variations may be neglected except in the buoyancy term (Spiegel and Veronis, 1959).

- The ambient air temperature is assumed constant. The model neglects air temperature stratification effects in the surroundings.

- Airflow through the system is assumed hydro dynamically and thermally fully developed.

- Hydro dynamic and thermal effects due to the experimental model inlet cone are not considered in the theoretical model.

3.1 Evaporative pads

The evaporative pads are further discretised as shown in figure 6
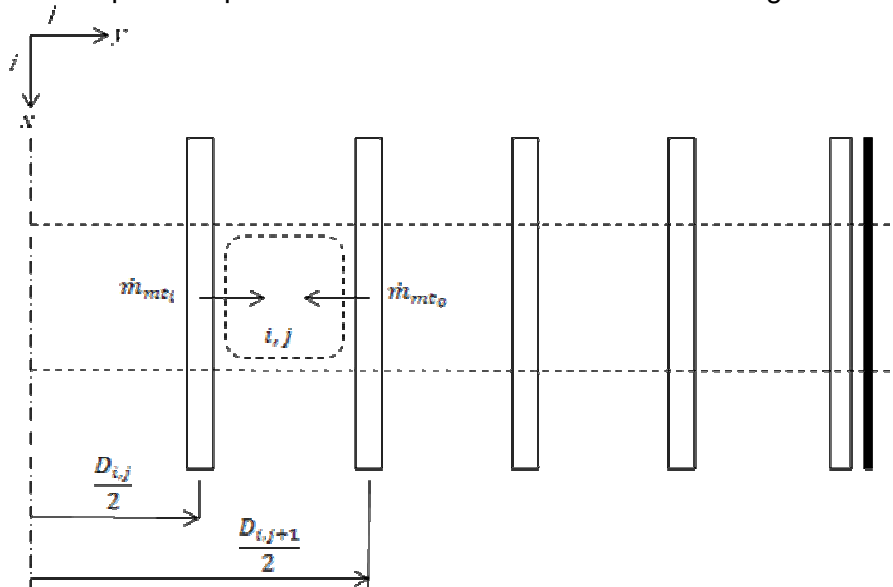

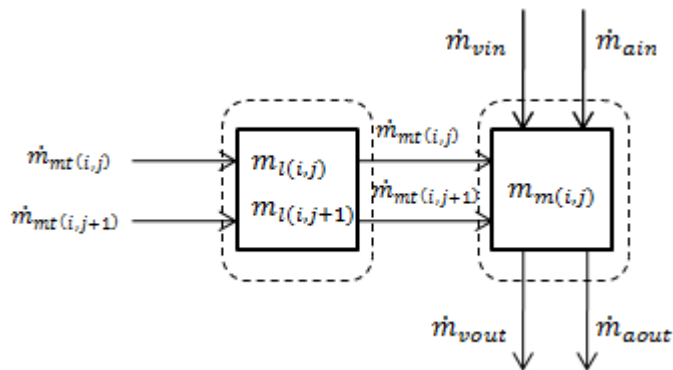
Figure 6 Mass transfer control volume
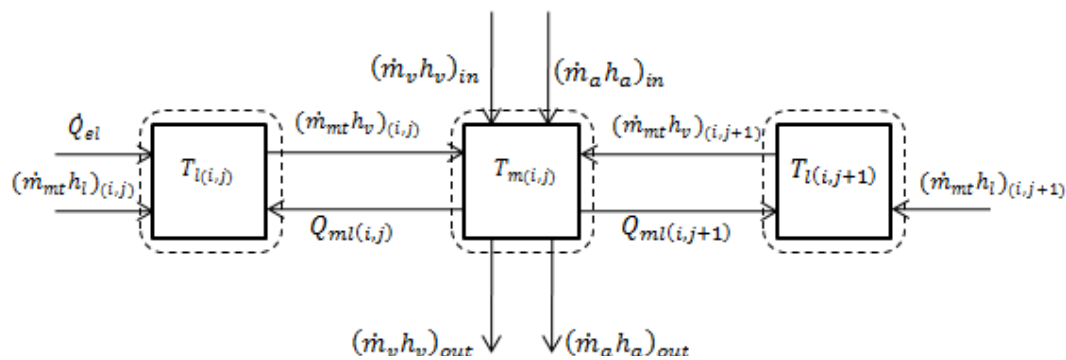
Figure 7 Conservation of mass control volume

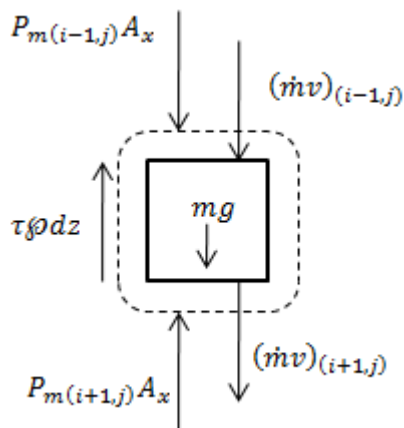Figure 8 Conservation of energy control volume

Figure 9 Conservation of momentum control volume

3.1.1 Mass Transfer

Evaporation from the concentric evaporator pads result in mass and thus energy transfer to the air. The mass transfer rate of vapour into the air $\dot{m}_{mt}$ as given by Cengel (2006) is

$$\dot{m}_{mt} = h_{mt} A_{mt} \left(\rho_{vsat@Tl} - \rho_{v@Tm} \right) \qquad 3.1$$

Where h_{mt} is the mass transfer coefficient, A_{mt} is the mass transfer area and $\rho_{vsat@Tl}$-$\rho_{vsat@Tm}$ is the mass concentration difference of water vapour across the control volume boundary. A cross section through an annular control volume depicting the adjacent, cylindrical evaporative pads is illustrated in Figure 6 .

Mass is transferred to each annular air control volume from the two enclosing wetted cylinders. The total vapour mass transfer rate to the air control volume is therefore the sum of the mass transfer rate from each evaporating surface.

$$\dot{m}_{mt(i,j)} = h_{mt(i,j)} A_{mt(i,j)} \left(\rho_{vsat@Tl(i,j)} - \rho_{v@Tm(i,j)} \right) +$$
$$h_{mt(i,j+1)} A_{mt(i,j+1)} \left(\rho_{vsat@Tl(i,j)} - \rho_{v@Tm(i,j)} \right) \tag{3.2}$$

Where

$$h_{mt(i,j)} = \frac{Sh_{(i,j)} D_{v\_a(i,j)}}{D_{(i,j)}}$$

$$A_{mt(i,j)} = \pi D_{(i,j)} dx_i$$

$$\rho_{vsat@Tl(i,j)} = \frac{P_{vsat@Tl(i,j)}}{R_v (T_l + 273.15)}$$

The Sherwood number Sh for fully developed laminar and turbulent flow is calculated in equations 3.3 and 3.4. The Schmidt Sc number is calculated in equation 3.5.

$$Sh_{(i,j)} = 3.66 \quad \text{for} \quad Re_{eff} < 2300 \tag{3.3}$$

$$Sh_{(i,j)} = 0.023 Re_{eff}^{0.8} Sc^{0.35} \quad \text{for} \quad Re_{eff} > 2300 \tag{3.4}$$

$$Sc_{(i,j)} = \frac{\mu_m}{\rho_m D_{va}} \tag{3.5}$$

According to White (2005) the effective Reynolds number for annular flow may be corrected by adjusting the Reynolds number with a factor ζ.

$$Re_{eff} = \frac{\rho_{m(i,j)} v_{avg(i,j)} D_{h(i,j)}}{\zeta \mu_m} \quad \text{where} \quad \zeta = \frac{(a-b)^2 (a^2 - b^2)}{a^4 - b^4 - \left(a^2 - b^2\right)^2 / \ln(a/b)}$$

with a and b being the outer and inner radii of the evaporation surfaces bordering the annular control volume respectively. The mass diffusivity of water vapour in air (Cengel, 2006) is given by equation 3.6.

$$D_{v\_a(i,j)} = \frac{1.87 \times 10^{-10} (T + 273.15)^{2.072} \times 101325}{P_{v(i,j)} + P_{a(i,j)}} \tag{3.6}$$

3.1.2 Heat Transfer

The ambient air entering the downdraught tower is cooled by the evaporation of water from the evaporative pads due to heat transfer from the air to the pads. The rate of heat transfer from the air to the liquid $\dot{Q}_{ml(i,j)}$ may be expressed by Newton's law of cooling (Cengel, 2006).

$$\dot{Q}_{ml(i,j)} = h_{ml} A_{s(i,j)} \left(T_{m(i,j)} - T_{l(i,j)} \right) \tag{3.7}$$

Where $T_{m(i,j)}$ is the mixture temperature, $T_{l(i,j)}$ is the liquid temperature, h_{ml} is the convection heat transfer coefficient and $A_{s(i,j)}$ is the heat transfer area (surface area of the evaporative pad being considered). According to Cengel (2006) the convection heat transfer coefficient may be calculated as shown in equation 3.8 where Nu is the Nusselt number, k is taken as the thermal conductivity of air and D_h is the hydraulic diameter where $D_h = D_{(i,j+1)} - D_{(i,j)}$.

$$Nu = \frac{h D_h}{k} \tag{3.8}$$

Flow through the annular space between the evaporative pads is associated with two Nusselt numbers, Nu_i for the inner surface and Nu_o for the outer surface (Cengel, 2006).

$$Nu_i = \frac{h_i D_h}{k} \qquad\qquad 3.9$$

$$Nu_o = \frac{h_o D_h}{k} \qquad\qquad 3.10$$

Where h_o and h_i are the convection heat transfer coefficients for the outside and inside surface of the bordering the annular space respectively. For fully developed laminar and turbulent flow the Nusselt numbers are given by equations 3.11 and 3.12, where Pr is the Prandtl number of air (Cengel, 2006).

$$Nu = 3.66 \qquad\qquad 3.11$$

$$Nu = 0.023 Re_{eff}^{0.8} Pr^{0.3} \qquad\qquad 3.12$$

Heat transfer from the environment to the liquid $\dot{Q}_{el(i,j)}$ is only considered for the outer evaporative pad. The outer pad borders the acrylic cylinder holding the evaporator cartridge in place. Newton's law for convection heat transfer from the environment to the outer evaporative pad may be rearranged as in equation 3.13 (Cengel, 2006).

$$\dot{Q}_{el(i,j)} = \frac{(T_e - T_{l(i,j)})}{R_{el}} \qquad\qquad 3.13$$

Where T_e is the ambient temperature, $T_{l(i,j)}$ is the liquid temperature and R_{el} is the convection R_{conv}, conduction R_{acr} and contact R_c thermal resistances combined. The thermal resistance is calculated in equation 3.14 where h_o is the convection heat transfer coefficient on the outside of acrylic shell, L_{acr} is the thickness of the acrylic shell, k_{acr} is the conduction heat transfer coefficient, h_c is the thermal contact conductance and A is the outside surface area of the acrylic shell. The thermal resistance network is shown in figure 10 is

$$R_{el} = R_{conv} + R_{acr} + R_c$$

$$R_{el} = \frac{1}{h_o A} + \frac{L_{acr}}{k_{acr} A} + \frac{1}{h_c A} \qquad\qquad 3.14$$

The acrylic shell is approximated as having a constant surface area in the radial direction seeing that it has a very small thickness compared to the diameter of the shell.
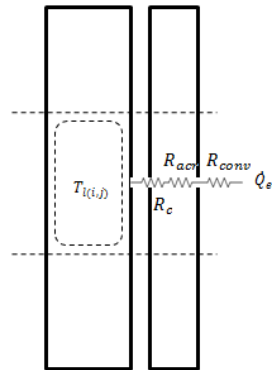

Figure 10 Thermal resistance network

3.1.3 Conservation of Mass

The law of conservation of mass for a fixed control volume with one dimensional inlets and outlets is given by equation 3.15 (White, 2005).

$$\frac{dm}{dt} = \Sigma \dot{m}_{in} - \Sigma \dot{m}_{out} \qquad\qquad 3.15$$

Where for the assumed one-dimensional flow $\dot{m} = \rho A_x v$. The conservation of mass principle for vapour and air is applied to the control volume depicted in figure 10 where the i's and j's are defined in Figure 6 and the adjacent liquid control volumes are depicted as a single control volume for convenience.

By making use of an explicit solution method and realising that $\dot{m} = \rho A_x v$ the new (at time t + Dt) mass in terms of the old (at time t) mass and mass flow rates for each of the control volumes (namely the liquid and the air consisting of dry air and water vapour) are given by equations 3.16 and 3.17.

$$m_{a(i,j)}^{new} = m_{a(i,j)} + \Delta t (\dot{m}_{ain} - \dot{m}_{aout})^{old} \tag{3.16}$$

$$m_{v(i,j)}^{new} = m_{v(i,j)}^{old} + \Delta t (\dot{m}_{vin} - \dot{m}_{vout})^{old} \tag{3.17}$$

where "old", for air has for convenience been omitted.

For upwind differencing, if $\dot{m}$ is positive i.e. ambient air enters the evaporator section from the top, $\dot{m}_{ain} = \dot{m}_{ain(i-1,j)}$, $\dot{m}_{vin} = \dot{m}_{vin(i-1,j)}$, $\dot{m}_{aout} = \dot{m}_{aout(i,j)}$ and $\dot{m}_{vout} = \dot{m}_{vout(i,j)}$. For a negative mass flow rate $\dot{m}$, $\dot{m}_{ain} = \dot{m}_{ain(i+1,j)}$, $\dot{m}_{vin} = \dot{m}_{vin(i+1,j)}$, $\dot{m}_{aout} = \dot{m}_{aout(i,j)}$ and $\dot{m}_{vout} = \dot{m}_{vout(i,j)}$ where "negative" implies that air inside the SCAPDEC loop enters the evaporative cartridge from the bottom and exits to the environment through the top of the evaporative cartridge.

3.1.4 Conservation of Energy

figure 8 depicts an air-vapour mixture control volume in the evaporator section with the two adjacent liquid control volumes. Equation 3.18 gives the conservation of energy applied to the liquid control volumes in Figure 8.

It is assumed that make-up water at a temperature T_l is supplied to each liquid control volume at the same rate as the evaporation of vapour into the air from that surface. The mass of the liquid control volume may therefore be assumed constant.

$$\frac{\Delta E}{\Delta t} = \frac{\Delta}{\Delta t}(m_l c_v T_l)$$
$$= \dot{Q}_{el} + \dot{Q}_{ml} + (\dot{m}_{mt} h_l)_{(i,j)} + (\dot{m}_{mt} h_l)_{(i,j+1)} - (\dot{m}_{mt} h_v)_{(i,j)} - (\dot{m}_{mt} h_v)_{(i,j+1)} \tag{3.18}$$

By using an explicit solution scheme the new liquid control volume temperatures can be calculated with equation 3.19.

$$T^{new}{}_{l(i,j)} = T^{old}{}_{l(i,j)}$$
$$+ \Delta t \left(\frac{Q_{el} + Q_{ml} + (m_{mt} h_l)_{(i,j)} + (m_{mt} h_l)_{(i,j+1)} - (m_{mt} h_v)_{(i,j)} - (m_{mt} h_v)_{(i,j+1)}}{m_{l(i,j)} c_v} \right) \tag{3.19}$$

Where $\dot{Q}_{el}$ is the rate of heat transfer from the environment to the liquid, $\dot{Q}_{ml}$ the rate of heat transfer from the air-vapour mixture to the liquid, h_l is the enthalpy of the make-up water and h_v the enthalpy of the water vapour. Conservation of energy is next applied to the air-water vapour mixture control volume in Figure 8.

$$\frac{\Delta}{\Delta t}(m_m c_v T_m) = m_m c_v \frac{dT}{dt} + c_v T_m \frac{dm}{dt}$$
$$= (\dot{m}_a h_a)_{in} + (\dot{m}_v h_v)_{in} - (\dot{m}_a h_a)_{out} - (\dot{m}_v h_v)_{out}$$
$$+ (\dot{m}_{mt} h_v)_{(i,j)} + (\dot{m}_{mt} h_v)_{(i,j+1)} - \dot{Q}_{ms} - \dot{Q}_{ml} \tag{3.20}$$

In equation 3.21 the new air-vapour mixture temperature for the control volume is calculated.

$$T_m{}^{new} = T_m{}^{old} + \Delta t \left(\frac{(\dot{m}h)_{in} - (\dot{m}h)_{out} - c_v T_m{}^{old}\frac{dm}{dt}}{m_{m(i,j)}c_v} \right) \tag{3.21}$$

Where

$$(\dot{m}h)_{in} = (\dot{m}_a h_a)_{(i-1,j)} + (\dot{m}_v h_v)_{(i-1,j)} + (\dot{m}_{mt} h_v)_{(i,j)} + (\dot{m}_{mt} h_v)_{(i,j+1)} \tag{3.22}$$

$$(\dot{m}h)_{out} = (\dot{m}_a h_a)_{(i,j)} + (\dot{m}_v h_v)_{(i,j)} + \dot{Q}_{ml} + \dot{Q}_{ms} \tag{3.23}$$

For upwind differencing and a positive mass flow rate, $\dot{m}_{a(i-1,j)}$ and $\dot{m}_{v(i-1,j)}$ are the mass flow rates of air and vapour into the control volume with $\dot{m}_{a(i,j)}$ and $\dot{m}_{v(i,j)}$ being the mass flow rates of air and vapour leaving the control volume.

3.1.5 Conservation of Momentum

The conservation of momentum applied to the control volume in Figure is given by equation 3.24.

$$\frac{\Delta(mv)_{(i,j)}}{\Delta t} = \left((\dot{m}v)_{(i,j)} - (\dot{m}v)_{(i+1,j)}\right) + \left(P_{m(i-1,j)} - P_{m(i+1,j)}\right)A_x$$
$$+ mg\sin\theta - \tau\wp dz \tag{3.24}$$

The cross sectional area of each control volume is assumed constant. Noting that $\dot{m} = \rho A_x v$, $\wp = \pi D$ and $G = A_x v$ equation 3.25 is divided by A_x and the shear stress due to friction expressed as $\tau_w = f\frac{\rho v^2}{8}$ (Cengel and Cimbala, 2006).

$$\frac{\Delta(mG/A_x^2)_{(i,j)}}{\Delta t} = \left(\frac{\rho_{(i-1,j)}G^2}{A_x A_{x(i-1,j)}} - \frac{\rho_{(i+1,j)}G^2}{A_x A_{x(i+1,j)}} \right) + \left(P_{m(i-1,j)} - P_{m(i+1,j)}\right)$$
$$+ \rho g dz \sin\theta - f\frac{\rho\pi D (G/A\_x)^2 dx}{8 A_x} \tag{3.25}$$

Equation 3.25 may now be integrated for all the control volumes around the natural circulation loop.

$$\sum_{i=1}^N \frac{\Delta(mG/A_x^2)_{(i,j)}}{\Delta t} = \sum_{i=1}^N \left(\frac{\rho_{(i-1,j)}G^2}{A_x A_{x(i-1,j)}} - \frac{\rho_{(i+1,j)}G^2}{A_x A_{x(i+1,j)}} \right) + (P_0 - P_{N+1})$$
$$+ \sum_{i=1}^N \rho_{(i,j)} L_{(i,j)} g \sin\theta - \sum_{i=1}^N f\frac{\rho\pi D \left(\frac{G}{A_x}\right)^2 (L_{(i,j)} + L_{equ(i,j)})}{8 A_x} \tag{3.26}$$

Due to the assumption of constant cross sectional area it is noted that all the intermediate pressure terms conveniently cancel out. In equation 3.26 dx has been replaced with $L_{(i,j)}$ and the minor losses are accounted for by the use of equivalent lengths. For a sharp inlet $L_{equ(i,j)} = 18 D_h$ (Batty and Folkman, 1983). Equation 3.26 may be simplified by applying the Boussinesq approximation where it is assumed that the density is essentially constant except in the buoyancy term (Spiegel and Veronis, 1959). The density in each control volume is calculated by means of the ideal gas approximation. A reference density $\bar{\rho}$ is determined at the ambient temperature and pressure.

$$\sum_{i=1}^N \frac{\Delta(mG/A_x^2)_{(i,j)}}{\Delta t} = \bar{\rho}g(L_0 - L_{N+1}) + \sum_{i=1}^N \left(\frac{\rho_{(i-1,j)}G^2}{A_x A_{x(i-1,j)}} - \frac{\rho_{(i+1,j)}G^2}{A_x A_{x(i+1,j)}} \right)$$
$$+ \sum_{i=1}^N \rho_{(i,j)} L_{(i,j)} g \sin\theta - \sum_{i=1}^N f\frac{\rho\pi D \left(\frac{G}{A_x}\right)^2 (L_{(i,j)} + L_{equ(i,j)})}{8 A_x} \tag{3.27}$$

From equation 3.27 it is seen that the rate of change of momentum in the natural circulation loop depend essentially on four terms. The first term in brackets X accommodates the difference in height between inlet and outlet. The second term MF takes into account the mass flux through the system. The driving term B which depend on the density and a retarding term due to friction F.

The volumetric flow rate through the system may be determined by equation 3.28.

$$G^{new} = G^{old} + \Delta t(X + MF + B - F)\sum_{i=1}^{N}\left(\frac{A_{x(i,j)}}{m_{(i,j)}}\right)$$ 3.28

Where

$$X = \bar{\rho}g(L_0 - L_{N+1})$$

$$MF = \sum_{i=1}^{N}\left(\frac{\rho_{(i-1,j)}G^2}{A_x A_{x(i-1,j)}} - \frac{\rho_{(i+1,j)}G^2}{A_x A_{x(i+1,j)}}\right)$$

$$B = \sum_{i=1}^{N}\rho_{(i,j)}L_{(i,j)}g\sin\theta$$

$$F = \sum_{i=1}^{N}f\frac{\rho\pi D\left(\frac{G}{A_x}\right)^2(L_{(i,j)} + L_{equ(i,j)})}{8A_x}$$

3.2 Rest of system

Similar equations may be derived for the rest of the system by applying the conservation of mass, energy and momentum as was done in section 3.1 to the control volumes given in figures 11, 12 and 13.
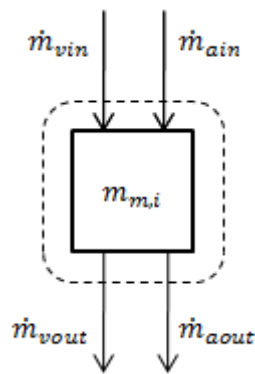
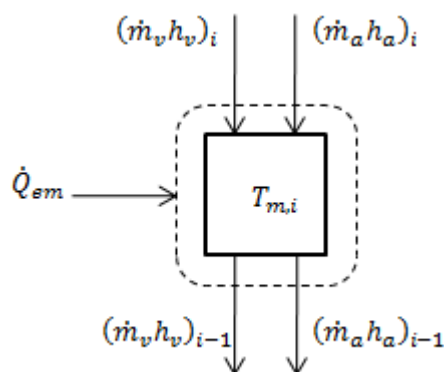
Figure 11 Conservation of mass control volume

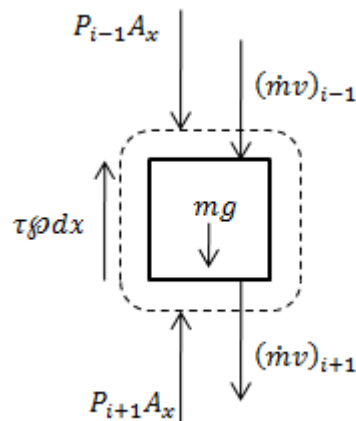Figure 12 Conservation of energy control volume

Figure 13 Conservation of momentum control volume

3.3 Solution Procedure

The stepwise solution procedure for the theoretical model, as implemented in the theoretical model, is outlined below:

(1) Define the initial values for all variables and set the boundary conditions.

(2) Calculate the rates of heat transfer from the incoming air to the evaporative pads (equation 3.7); from the environment to the air-vapour mixture (equation 3.13) and the rate of heat transfer from the solar chimney to the mixture.

(3) Calculate the new air and vapour masses in each control volume by applying the finite difference equation for the conservation of mass using equations 3.16, 3.17.

(4) The new mixture temperatures are calculated by applying the finite difference equation for the conservation of energy, given by equation 3.21, to each control volume.

(5) Calculate the rates of mass transfer from the evaporative pads into the air by making use of equation 3.2.

(6) The new liquid temperature in the evaporator pads are calculated by applying the finite difference formulation for the conservation of energy (equation 3.19) to each "liquid" control volume.

(7) The finite difference formulation for the conservation of momentum is applied to the system in order to determine the volumetric Flow Rate G in equation 3.28.

(8) Set the "old" values (calculated at time t) equal to the "new" values (calculated at $t + \Delta t$).

(9) Write output data to a text file.

(10) Steps (2) to (8) are repeated until a predefined number finite time steps are reached.
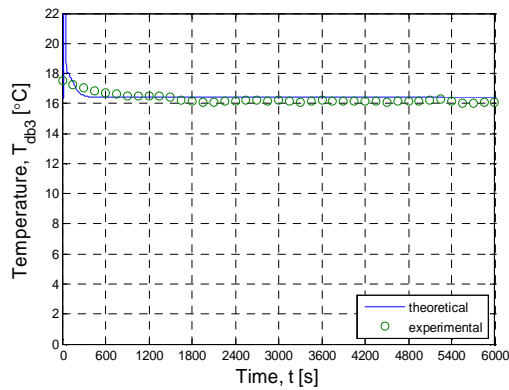
4 Results

Figures 14 to 16 give the volumetric flow rate through the system and the dry bulb temperature at the exit of the evaporator cartridge T_{db2} for different inlet air temperatures and relative humidity's T_{db1} and ϕ_1.
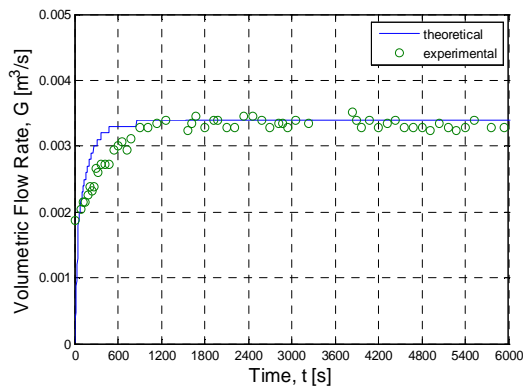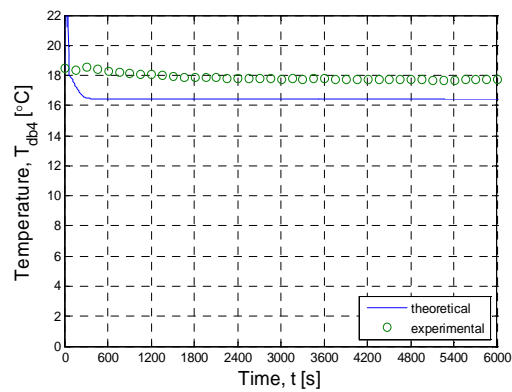

(a) Volumetric Flow Rate G
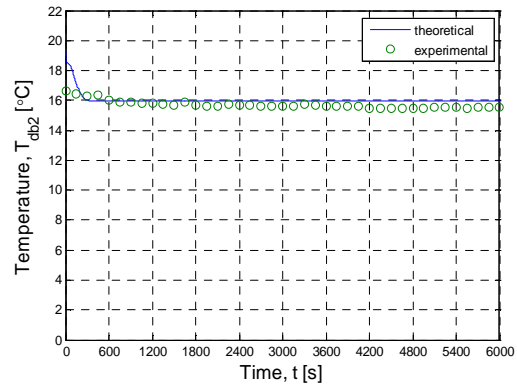
(b) Temperature T_{db2}

(c) Temperature T_{db3}

(d) Temperature T_{db4}

(e) Temperature T_{db5}

Figure 14 SCAPDEC volumetric flow rate and temperatures at a low air-heater heated solar chimney with $T_{db1} = 18.3$ ºC and $\phi_1 = 67\%$
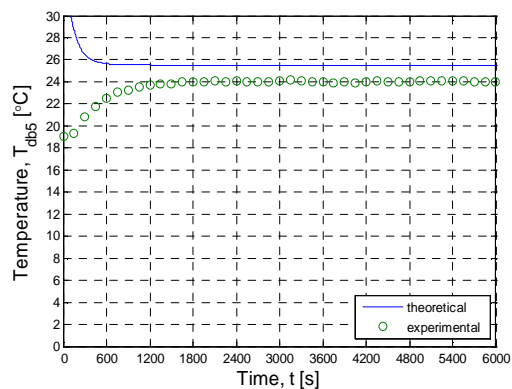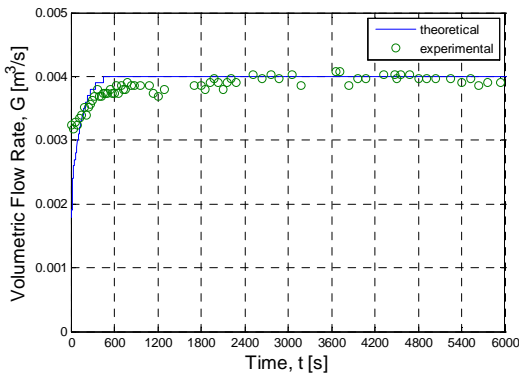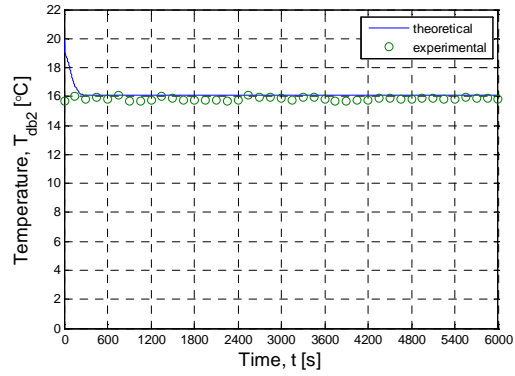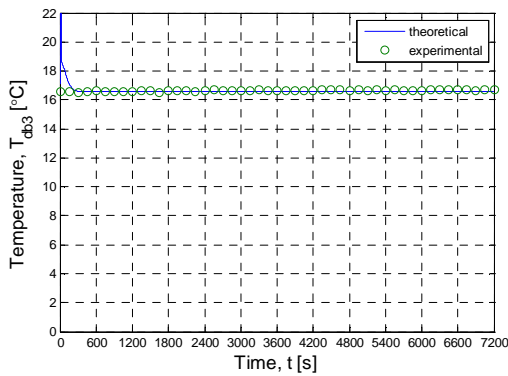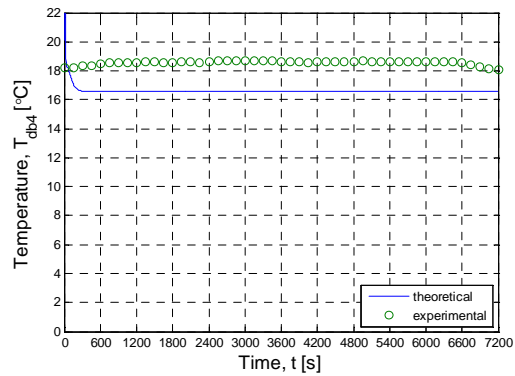
(a) Volumetric Flow Rate G

(b) Temperature T_{db2}

(c) Temperature T_{db3}

(d) Temperature T_{db4}

(e) Temperature T_{db5}

Figure 15 SCAPDEC volumetric flow rate and temperatures at a high air-heater heated solar chimney with T_{db1} = 19.0 ºC and $\phi1$ = 74%

5 Discussion and Conclusions

The use of passive cooling strategies to achieve thermal comfort in buildings could considerably alleviate the operational energy demand of buildings. That is without the use of any mechanical parts such as pumps and active control strategies and also without the use of any fossil fuel produced energy. A literature survey revealed that the need for passive cooling strategies is greatest in developing countries where modern building design has in many cases superseded indigenous architecture.
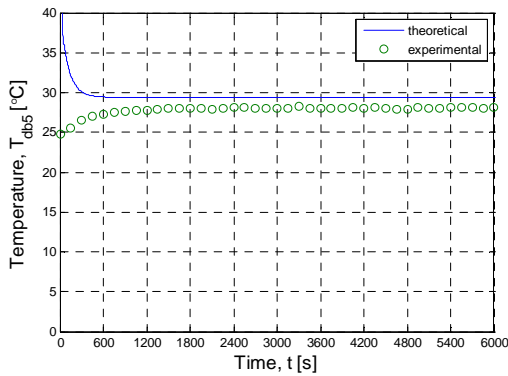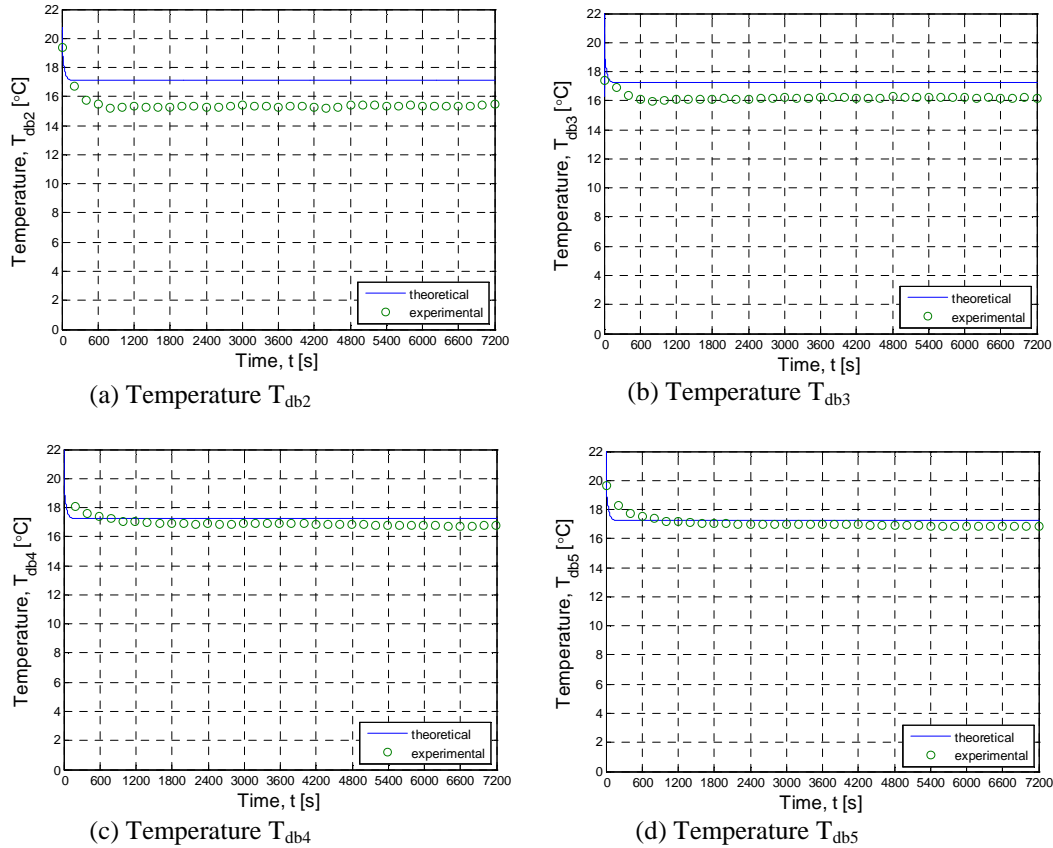
(a) Temperature T_{db2}

(b) Temperature T_{db3}

(c) Temperature T_{db4}

(d) Temperature T_{db5}

Figure 16 SCAPDEC volumetric flow rate and temperatures for a forced-draught with T_{db1} = 19.8 ⁰C and ϕ_1 = 72%

A solar chimney augmented passive downdraught evaporative cooling (SCAPDEC) system was identified as a promising approach to achieving thermal comfort in buildings. A SCAPDEC system consists of a downdraught tower incorporated into one side of a building, where air is cooled through the evaporation of water. The cool air moves down the tower and enters the living space. On the other side of the building a solar chimney induces an upward draught, removing stagnant air from the building. It has been proposed that either one of the towers may be operated separately in the case where the prevailing ambient conditions are not suitable for the operation of one of the towers.

Empirical relations to predict the volumetric flow rate and temperature of the air entering the living space were found in the literature and presented. Recent studies making use of commercial CFD packages to predict SCAPDEC system performance have been conducted.

Barozzi et al. (1992) reported that results obtained from a CFD analysis on a solar chimney incorporated in to the roof structure of a building compared well with results obtained from a 1:12 scale model test. From the literature survey it was concluded that current methods for predicting the performance of SCAPDEC systems rely predominantly on empirical methods. Insufficient computational power was identified as a possible pitfall in using CFD as a design tool for SCAPDEC systems in the developing world.

The objective of the current study was to develop an experimentally validated, one dimensional, finite difference theoretical model to assimilate the operation of SCAPDEC systems. In order to develop the proposed theoretical model a few simplifying assumptions had to be made, with the most significant being; a uniform property distribution being assumed in each control volume; only buoyancy driven ventilation is considered and wind

induced ventilation is omitted and finally the Boussinesq approximation is applied in solving the momentum equation. The theoretical model was presented section 3 by formulation of the finite difference equations for the conservation of mass, momentum and energy.

The experimental SCAPDEC setup used to validate the theoretical model was introduced in section 4 of the report. In short, the experimental model consists of essentially three acrylic tubes joined by 90 degree PVC elbows to approximate the PDECT, living space and solar chimney. At the top of the downdraught tube is mounted a removable evaporative cartridge consisting of eight concentric, cylindrical cotton pads supported by a wire frame. A simple tube-in-tube heat exchanger, fashioned from acrylic sheet, is used in conjunction with an air heater to approximate a solar chimney.

A comparison of the experimental and theoretical results was presented in section 5. Velocity measurements were taken at the bottom of the downdraught tube in order to determine the velocity profile in the pipe at various centreline velocities. The measured velocity profiles were compared with velocity profiles predicted by fully developed laminar theory as well as the one-seventh power law for fully developed turbulent flow. It was observed that the one-seventh power law approximated the measured velocity profiles exceptionally well. It was concluded that the use of the one-seventh power law to determine the average velocity and flow rate from a measured centreline maximum velocity is a valid assumption.

Overall, the theoretical model seems to capture the behaviour of the experimental model exceptionally well. From the SCAPDEC test results presented in sections 5.2 and 5.3 it was concluded that the volumetric flow rate responds very well to an increased energy input into the solar chimney when the air heater power setting was changed. The theoretical model was observed to predict both the initial, transient and steady state volumetric flow rates very well. The predicted dry bulb temperature after the evaporator T_{db2} and before the living space T_{db3} was also seen to correspond well with the measured temperatures. Some initial instability in the predicted temperatures was observed before the temperatures stabilized. Reasons for the instability were postulated in section 5.2. From the results of the two SCAPDEC tests it was suggested that the calculated convection heat transfer coefficients for the solar chimney may be slightly optimistic. The assumption of omitting heat transfer from the environment to the living space proved not to be very good. In both SCAPDEC tests the measured temperature after the living is observed to be well above the predicted value.

From the results of the forced draught test it was seen that the theoretical model under predicted the temperature drop across the evaporator cartridge. It was put forward that the fan caused the incoming air to be highly turbulent therefore assisting convection heat transfer from the air to the evaporative pads. The theoretical model did not account for the fan induced turbulence. From the solar chimney test results presented in sections 5.5 and 5.6 it was observed that the theoretical model over predicted the volumetric flow rate through the system. The predicted temperature of the air leaving the solar chimney T_{db5} was also seen to be higher than the measured values. The above two observations correspond with the suspicion that the convection coefficients applied in the solar chimney heat transfer model might have been too high.

A comparison of the flow rates measured during the SCAPDEC and SC tests at the low air heater power setting was given in figure 14. Since the two tests were conducted on the same day under similar ambient conditions it seemed prudent to compare the two sets of results in order to gauge the solar chimney's contribution with regards to the volumetric flow rate through the system. It was observed that the volumetric flow rate depended for the most part on the heat input to the solar chimney. This observation conflicts with the findings of Cunningham, Mignon and Thompson (1986) who reported that the flow rate through their full scale SCAPDEC system depended almost exclusively on the temperature difference

between the air inside and outside the evaporative cooling tower. It is suspected that this discrepancy might be due to scaling effects that will be further discussed in the recommendations section. During the extended test run, air was observed to flow through the system even before the air heater was switched on. This observation affirms Cunningham, Mignon and Thompson's (1986) assertion that either one of the towers may be used when the ambient conditions are not fit for the operation of the other.

From the sensitivity analysis conducted in section 5.7 it was concluded that the predicted temperature after the evaporator cartridge T_{db2} is very robust to parameter change. The flow rate did however respond to these parameter changes. A similar observation was made during an extended experimental run where the air heater was run at a low heating setting before it was switched to high. The measured flow rate responded almost immediately to the change in heat input while T_{db2} showed little change. By varying the control volume sizes it was determined that the theoretical solution was grid independent.

Considering the results of the current investigation it must be concluded that the one dimensional finite difference model successfully captures the operation of the laboratory scale SCAPDEC system.

6 Recommendations

From the results presented it was clearly observed that the assumption of neglecting heat transfer from the environment to the air-vapour mixture in the living space is not valid. The theoretical model should therefore be modified to include heat transfer to the living space.

It is further suspected that the convection heat transfer coefficients for the tube-in-tube heat exchanger are too high. Further investigation of these coefficients should be considered. An in-depth investigation on the hydro dynamic effects the inlet cone has on the incoming air should be conducted. As was mentioned in section 5.3 no discernable effect on the flow rate was observed by adjusting the inlet cone height. It was observed during the experimental procedure that hot air exiting the SCAPDEC model is drawn straight back into the loop. As explained in section 4, this problem was anticipated and provision was made to counteract hot air from being drawn back into the model. It is proposed that a bigger divider be put up between the solar chimney and downdraught tower.

Similar ambient conditions prevailed during all of the experimental runs. The theoretical model should be validated at a wider range of ambient temperature and relative humidity. The energy transferred from the air heater to the air-vapour mixture should be compared to the achievable heat transfer from solar radiation in a practical solar chimney of similar size. It was found that the solar chimney provides the majority of the driving force for air flow through the system. It was mentioned in section 6 that this observation is in conflict with findings made by Cunningham, Mignon and Thompson's (1986). It is proposed that the discrepancy is due to the experimental model not being geometrically scaled with an actual building. As stated in the experimental setup description provided in section 4, the modular model design would allow for a more representative "living space" to be included. Further research on the up-scaling to a full scale SCAPDEC model should be considered.

NOMENCLATURE

A area, m^2

A_s surface area, m

A_x cross sectional area, m^2

a outside radius, m

b inside radius, m

c_v specific heat at constant volume, J/kg.K

D diameter, m

D_{v_a} mass diffusivity of water vapour in air, m^2/s

f friction factor

G volumetric flow rate, m^3/s

Gr Grashof

g   gravitational acceleration, m/s^2

h   specific enthalpy, J/kg

h_{ht} convection heat transfer coefficient, W/m^2.K

h_{mt} mass transfer coefficient, m/s

k thermal conductivity, W/m.K

L length, m

m mass, kg

$\dot{m}$ mass flow rate, kg/s

Nu Nusselt number

P pressure, Pa

$\wp$ perimeter, m

$\dot{Q}$ heat transfer rate, W

Pr Prandtl number

R thermal resistance, K/W

Re Reynolds number

Sc Schmidt number

Sh Sherwood number

T temperature, ºC

t time, s

v velocity, m/s

V volume, m^3

Greek letters

ζ Reynolds number correction factor

θ angle

μ dynamic viscosity, kg/m.s

ρ density, kg/m^3

τ shear stress, N/m^2

ϕ relative humidity

Subscript

a	air
acr	acrylic
avg	average
$conv$	convection
c	contact
db	dry bulb
eff	effective
equ	equivalent
e	environment
ht	heat transfer
in	incoming
i	inside
i	lengthwise control volume
j	radial control volume
l	liquid
m	mixture
max	maximum
mt	mass transfer
out	outgoing
o	outside
sat	saturated
v	vapour
w	water
wb	wet bulb

REFERENCES

Barozzi, G.S., Imbabi, M.S.E., Nobile, E., Sousa, A.C.M. 1992. Physical and numerical modelling of a solar chimney-based ventilation system for buildings. *Building and Environment* 27.4: 443

Batty, J.C., Folkman, S.L. 1983. *Food Engineering Fundamentals.* Wiley: New York.

Cengel, Y.A. 2006. *Heat and mass transfer: A practical approach.* McGraw -Hill: New York.

Cengel, Y.A., Boles, M.A. 2007.*Thermodynamics: An engineering Approach. 6th ed.* McGraw - Hill: New York.

Cengel, Y.A., Cimbala, J.M. 2006. *Fluid Mechanics: Fundamentals and Applications.* 1st ed. McGraw –-Hill: Singapore.

Chakraborty, J., Fonseca, E. 2005. Analysis and evaluation of a passive evaporative cool tower in conjunction with a solar chimney. *Proceedings from the 22nd Conference on Passive and Low Energy Architecture*, Beirut, 13-16 November 2005. Lebanon.

Chalfoun, N.V. 1997. Design and application of natural down-draught evaporative cooling devices. *Proceedings of the 26th American Solar Energy Society (ASES) and the 22nd National Passive Solar Annual Conference. Washington, DC, 25-30 April 1997. USA.*

Cunningham, W.A., Mignon, G.V., Thompson, T.L. 1987. Establishing feasibility for providing passive cooling with solar updraft and evaporative downdraft chimneys. Final Report. The Environmental Research Laboratory, University of Arizona, Tucson.

Cunningham, W.A., Mignon, G.V. 1986. Establishing feasibility for providing passive cooling with solar updraft and evaporative downdraft chimneys. Progress Report. The Environmental Research Laboratory, University of Arizona, Tucson.

Dobson, R.T., le Grange, F. 2009. Mathematical modelling and verification of a passive downdraught evaporative cooling tower. Mechanical Project 478. Final Report, Department Mechanical and Mechatronic Engineering, Stellenbosch University.

Douglas, J.F., Gasiorek, J.M., Swaffield, J.A. 1995. *Fluid Mechanics*. 3rd ed. Wiley: New York

Erell, E., Pearlmutter, D., Etzion, Y. 2007. A multi-stage down-draft evaporative cool tower for semi-enclosed spaces: Aerodynamic performance. *Solar Energy* 82.2008: 420-429

Etzion, Y., Pearlmutter, D., Erel, E., Meir, I.A. 1997. Adaptive architecture: integrating low-energy technologies for climate control in the dessert. *Automation in Construction*. 6.1997: 417-425

Givoni, B. 1993. Semi-empirical model of a building with a passive evaporative cool tower. *Solar Energy*. 50.5:425-434

Kang, D., Strand, R.K. 2009. Simulation of passive down-draught evaporative cooling (PDEC) systems in energyplus. *Proceedings of Eleventh International IBPSA Conference*, Glasgow, 27-30 July 2009. Scotland: Building Simulation.

Liu, P., Lin, H., Chou, J. 2009. Evaluation of buoyancy-driven ventilation in atrium buildings using computational fluid dynamics and reduced-scale air model. *Building and Environment*. 44.2009: 1970-1979

Maerefat, M., Haghighi, A.P. 2010. Natural cooling of stand-alone houses using solar chimney and evaporative cooling cavity. *Renewable Energy*. 35.2010: 2040-2052

Pearlmutter, D., Erel, E., Etzion, Y., Meir, I.A. 1996. Refining the use of evaporation in an experimental down-draft cool tower. *Energy and Building*. 23.1996:191-197

Spiegel, E.A., Veronis, G. 1959. On the Boussinesq approximation for a compressible fluid. [Online]. Available: http://adsabs.harvard.edu/abs/1960ApJ...131...442S.
[2010, February 10]

Ssekibuule, R., Lakuma, J., Ngubiri, J. 2007. Computational resource optimization in Ugandan tertiary institutions. [Online].
Available: http://dspace.mak.ac.ug/handle/123456789/461.
[2010, September 28]

Thompson, T.L., Chalfoun, N.V., Yoklic, M.R. 1994. Estimating the performance of natural draft evaporative coolers. *Energy Convers. Mgmt*.
35.11: 909-915

Versteeg, H.K., Malalasekera, W. 2007. *An introduction to computational fluid dynamics: The finite volume method*. 2nd ed. Pearson: London

White, F.M. 2005 *Fluid Mechanics*, 5th ed. McGraw-Hill: New York.

Wong, H.Y. 1997. *Handbook of essential formulae and data on Heat Transfer for Engineers*. Longman: New York.